



**HAL**  
open science

# Real-space fluctuations of effective exchange integrals in high-Tc cuprates

Sébastien Petit, Marie-Bernadette Lepetit

► **To cite this version:**

Sébastien Petit, Marie-Bernadette Lepetit. Real-space fluctuations of effective exchange integrals in high-Tc cuprates. EPL - Europhysics Letters, 2009, 87 (6), pp.67005. <10.1209/0295-5075/87/67005>. <hal-00421221v2>

**HAL Id: hal-00421221**

**<https://hal.science/hal-00421221v2>**

Submitted on 13 Nov 2009

**HAL** is a multi-disciplinary open access archive for the deposit and dissemination of scientific research documents, whether they are published or not. The documents may come from teaching and research institutions in France or abroad, or from public or private research centers.

L'archive ouverte pluridisciplinaire **HAL**, est destinée au dépôt et à la diffusion de documents scientifiques de niveau recherche, publiés ou non, émanant des établissements d'enseignement et de recherche français ou étrangers, des laboratoires publics ou privés.



HAL Authorization

---

# Real-space fluctuations of effective exchange integrals in high- $T_c$ cuprates

SÉBASTIEN PETIT and MARIE-BERNADETTE LEPETIT

*CRISMAT, ENSICAEN-CNRS UMR6508, 6 bd. Maréchal Juin, 14050 Caen, FRANCE*

PACS 74.62.Dh – Effects of crystal defects, doping and substitution

PACS 75.30.Et – Exchange and superexchange interactions

PACS 71.10.Fd – Lattice fermion models (Hubbard model, etc.)

**Abstract.** - We present ab-initio calculations of effective magnetic exchange,  $J$ , as well as Hubbard parameters ( $t$ ,  $U$  and  $\delta\varepsilon$ ) as a function of the local distribution of doping atoms for the high- $T_c$  superconducting  $(\text{Ca}_x\text{La}_{1-x})(\text{Ba}_{1.75-x}\text{La}_{0.25+x})\text{Cu}_3\text{O}_y$  family. We found that both the exchange and the energies of the magnetic orbitals are strongly dependant on the local dopant distribution, both through the induced modification of the apical oxygen location and of the induced local electrostatic potential. The  $J$  real-space map, for a random distribution of dopants, positively compares with observed STS gap inhomogeneity maps. Similarly, the orbital energy fluctuations induce weak charge inhomogeneities on copper sites, that can be positively compared with the observed LDOS inhomogeneities. These results clearly support an extrinsic origin of both the gap inhomogeneities and LDOS.

---

Since their discovery by Müller in 1986 [1], high- $T_c$  superconductors have been the subject of an extensive research activity, both experimentally and theoretically. Recently, the question of the spatial (in)homogeneities of the superconducting state has attracted a lot of attention. Indeed, in the recent years, the improvement and development of the tunneling microscopy techniques such as Scanning Tunneling Spectroscopy (STS) have allowed the access to spatial imaging of quantities such as the density of states and the superconducting gap. Using these techniques, nanoscale spatial inhomogeneities of the gap amplitude were observed [2]. Strong fluctuations of the superconducting gap or even suppression of the superconductivity was found within islands of typical size of one nanometer in the  $\text{Bi}_2\text{Sr}_2\text{CaCu}_2\text{O}_{8+\delta}$  (Bi-2212) compound at 4.2K, that is far below the critical temperature [3]. The origin of these gap inhomogeneities is quite controversial, however crucial since some models link the high value of  $T_c$  to electronic phases separation or disorder. The controversy opposes authors defending the idea that this is an intrinsic feature of the superconducting state [3–5], to authors defending the idea of an extrinsic origin [6], linked to the chemical inhomogeneities. The first issue is directly related to the models originating the high- $T_c$  superconductivity in electronic phases separation [7]. Indeed, in such a case, the gap inhomogeneities would be a pure electronic

effect in an otherwise (chemically and structurally) homogeneous system. The second issue emphasizes the role of the always present chemical disorder resulting from the doping process out of the Mott-Hubbard insulating parent system.

Despite the unknown origin of high- $T_c$  superconductivity it is widely accepted that the antiferromagnetic correlations play an important role in its onset, either as a competing phase [8] or as a pairing mechanism [9]. Some authors even claim a direct scaling of the critical temperature with the effective magnetic exchange,  $J$ , between adjacent copper atoms [10, 11]. In any case  $J$  plays a central role in the superconductivity onset and thus its fluctuations as a function of the chemical and structural inhomogeneities is expected to yield valuable new insight on the origin (intrinsic or extrinsic) of the observed gap and  $T_c$  spatial fluctuations.

The present work proposes to study the local fluctuations of the effective exchange integral,  $J$ , as a function of the chemical and structural disorder in the  $(\text{Ca}_x\text{La}_{1-x})(\text{Ba}_{1.75-x}\text{La}_{0.25+x})\text{Cu}_3\text{O}_y$  (CLBLCO) copper oxides family. Indeed, this family presents two determinant characteristics, (i) the effect of hole doping and of chemical disorder is decoupled <sup>1</sup> (ii) structural informa-

---

<sup>1</sup>A simple formal charges analysis shows that the doping in the CLBLCO family is independent of the amount of calcium,  $x$ , in-

tions on the local distortions as a function of the chemical disorder are available [12].

For this purpose we used the CAS [13]+DDCI [14] (Complete Active Space + Difference Dedicated Configurations Interaction) quantum chemical spectroscopy method on embedded fragments. Indeed, this method is presently the most reliable and accurate one for the determination of effective magnetic integrals. It proved its efficiency on copper oxides superconductors and predicted the  $J$  values within experimental accuracy for a large number of such compounds [10].

The CAS+DDCI method is an exact diagonalization method within a selected set of electronic configurations, specifically chosen so that to properly treat (i) the strong electronic correlation within the set of magnetic orbitals and (ii) the screening effects on the all magnetic configurations. The orbital space is thus divided into three subsets : the **occupied orbitals** set spanning orbitals always doubly-occupied in the reference configurations (the CAS), the **active orbitals** set for which all possible orbital occupations and spins are found in the CAS configurations and the **virtual orbitals** set spanning orbitals always remaining empty in the CAS configurations. If the active orbitals are defined as the magnetic orbitals of the copper atoms, the CAS definition will thus insure the proper treatment (by exact diagonalization) of the correlation effects within them. The screening effects are then treated by adding to the diagonalization space all single and double excitations, on all CAS configurations, that participate to the excitations energies at the second order of the quasi-degenerate perturbation theory.

The embedded fragments are divided into a quantum part and a bath. The quantum part includes the magnetic atoms (copper atoms), the ligands mediating the interaction as well as the first coordination shell of magnetic and ligands fragments. The bath is built in order to reproduce the main effects of the rest of the crystal on the quantum part, that is the Madelung potential and the exclusion effects. The latter corresponds to the orthogonalisation of the quantum fragment orbitals to the orbitals of the rest of the crystal. This effect is usually taken into account through total ions pseudo potentials [15] (TIPs) located at the crystallographic positions of the first coordination shell of the quantum fragment. The former is reproduced using a set of renormalized charges.

The  $(\text{Ca}_x\text{La}_{1-x})(\text{Ba}_{1.75-x}\text{La}_{0.25+x})\text{Cu}_3\text{O}_y$  compounds with  $0.1 \leq x \leq 0.4$  and  $6.8 \leq y \leq 7.25$  are high temperature double-layers superconductors belonging to the YBCO group. As in the layered YBCO structure, the CLBLCO compounds are built from two different types

---

roduced in the compound ; the hole doping only depends on the oxygen concentration  $y$ . Two different copper oxide planes are crystallographically present in CLBLCO family : the superconducting ones, associated with crystallographic Cu II sites, that do not see much fluctuations of their oxygen composition and the non superconducting ones, associated with Cu I sites, with a  $y - 6$  oxygen composition.

of copper planes : (i) two  $\text{CuO}_2$  superconducting layers corresponding to the Cu II crystallographic sites (see ref. [12]) separated by randomly distributed calcium and lanthanum ions (named  $\text{La}_Y$ ), and (ii) basal  $\text{CuO}_{y-6}$  layers, corresponding to the crystallographic Cu I coppers. In the latter planes, the oxygen atoms (named  $\text{O}_\alpha$ ) are randomly distributed along the Cu–Cu bonds. Let us note that on the contrary to the YBCO compounds, no extended CuO chains are observed in these Cu I layers. The YBCO Ba sites are randomly occupied with barium and lanthanum ions (named  $\text{La}_{\text{Ba}}$ ). Associated with the apical oxygen atoms ( $\text{O}_c$ ), they form layers in between the Cu II and Cu I planes.

From the above crystallographic data [12] one can spot four origins for the chemical and structural disorder. (i) The random distribution of the Ba and  $\text{La}_{\text{Ba}}$  ions in the YBCO Ba site. (ii) The in plane displacements of the  $\text{O}_c$  (apical) and  $\text{O}_\alpha$  (Cu I layers) oxygen atoms as a function of the doping ion on the YBCO Ba site. Indeed, the  $\text{Ba}^{2+}$  ions are 20% larger than the  $\text{La}^{3+}$  ones. (iii) The random distribution of Ca and  $\text{La}_Y$  ions in the YBCO Y site. (iv) The random distribution of the  $\text{O}_\alpha$  ions.

It is usually accepted that the exchange couplings are mainly sensitive to the geometry of the coppers first coordination shells. In the CLBLCO family this geometry is controlled by the YBCO Ba sites occupation [12]. In the present work we thus focused on the effect of this degree of freedom, and averaged the electrostatic effects induced by the  $\text{O}_\alpha$  positional disorder as well as those induced by the Ca /  $\text{La}_Y$  chemical disorder.

We computed the effective exchange  $J$  between nearest neighbor (NN) copper atoms as well as the parameters of a Hubbard model (that is  $t$ ,  $U$  and  $\delta\varepsilon$ ) as a function of the local ion distribution on the YBCO Ba site. Following the above specifications for building the embedded fragment, the quantum part was reduced to a  $\text{Cu}_2\text{O}_9$  fragment surrounded by 6  $\text{Cu}^{2+}$  and 10  $\text{O}^{2-}$  TIPs in the  $\text{CuO}_2$  plane, 2 Cu I TIPs on top of the apical oxygens, 6  $(\text{Ca}/\text{La})^{(3-x)+}$  averaged TIPs on the YBCO Y sites, and 6 either  $\text{Ba}^{2+}$  or  $\text{La}^{3+}$  on the YBCO Ba sites, as pictured in figure 1. Distributing  $\text{Ba}^{2+}$  and  $\text{La}^{3+}$  ions in all possible manners in the 6 available positions next to the  $\text{Cu}_2\text{O}_9$  fragment, one finds 24 non-equivalent configurations. The probability of each distribution depends on the value of  $x$ . According to the X-Ray structural data of reference [12], each of these configurations is associated with a specific displacement of the apical oxygens of the  $\text{Cu}_2\text{O}_9$  fragment as well as a specific localization of the  $\text{Ba}^{2+}$  and  $\text{La}^{3+}$  ions, according to their nature. For each configuration, the atomic positions used in our calculations (both for the  $\text{Cu}_2\text{O}_9$  fragment and the TIPs) were extracted from the experimental data of reference [12]. The set of renormalized charges was built so that to reproduce the “long” range part of the Madelung potential of the crystal, averaged over ions disorder. The renormalization factors from the formal charges were computed along the method of reference [16]. We imposed the nullity of all multipolar mo-

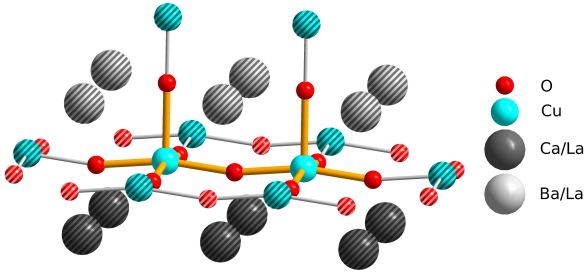


Fig. 1: (Color online) Schematic representation of the quantum part and TIPs (dashed) of the embedded fragments. The difference between the quantum part and the TIPs is emphasized by used of undashed/dashed atoms and large/small bond lines.

ments up to order 8. It resulted a set of 90616 renormalized charges. The charges locations were set to the experimental crystallographic positions given in reference [12], without the local displacements associated with a specific local ions configuration. The ions nominal charges were taken as the averaged nominal charges on the crystallographic site ; that is for the superconducting  $\text{CuO}_2$  layers and related apical oxygens :  $\text{Cu} \equiv 2+$ ,  $\text{O} \equiv 2-$ , for the doping  $\text{CuO}_{y-6}$  layers :  $\text{Cu} \equiv 2+$ ,  $\text{O} \equiv \eta \times 2-$ , where  $\eta$  is the site occupation probability in the AFM parent system, for the Ba/La and Ca/La layers  $2.125 + x/2$  and  $3 - x$ . The Madelung potential obtained from this set of renormalized charges exhibited an error smaller than 1 meV on any site of the quantum part. We also ran test calculations in order to verify that (i) the charge modifications associated with the doping from the AFM parent, (ii) as well as the actual ion distribution in those far away layers, do not affect the results in any significant way (error bar 2-3 meV).

We computed the  $J$ ,  $t$ ,  $U$  and  $\delta\varepsilon$  parameters for the 24 distributions, for  $x = 0.1$  and  $x = 0.4$  and the hole doping parameter  $y$  associated with the maximal critical temperature given in reference [12] — that is  $y = 7.158$ ,  $T_c = 52.6\text{K}$  for  $x = 0.1$  and  $y = 7.174$ ,  $T_c = 80.3\text{K}$  for  $x = 0.4$ .

Figure 2 presents the probability of each  $J$  value occurrence and figure 3 displays the resulting real-space map of magnetic exchange obtained for a random distribution of the Ba and La ions in the YBCO Ba sites. One sees immediately that the  $J$  values are spread over a range wider than 20 meV for each system despite the fact the Cu–O–Cu buckling angle does not depend on the Ba/La<sub>Ba</sub> distribution. Indeed, the buckling angle is only system dependant. For a given compound, the  $J$  distribution is thus independent of it, while this is the contrary for the average exchange value,  $\bar{J}$ . One finds, for the two studied compounds,  $\bar{J}_{x=0.1} = -110\text{meV}$  for a buckling angle of  $\theta = 167.2^\circ$  and  $\bar{J}_{x=0.4} = -132\text{meV}$  for  $\theta = 170.0^\circ$ . Let us note that the variation of  $\bar{J}$  with  $\theta$  is as expected, that is the super-exchange term increases with the overlap between the magnetic Cu  $3d_{x^2-y^2}$  orbitals and the bridging in-plane oxygen  $2p$  orbitals (i.e. with  $\cos^2(\theta - \pi)$ ).

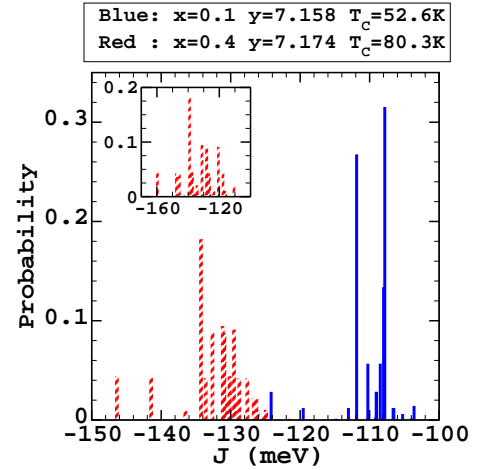


Fig. 2: (Color online) Probability of effective exchange values. Antiferromagnetic exchange  $J$  are taken negative. The inset shows the probability of occurrence for effective exchange values when the atomic displacements (induced by the nature of the surrounding Ba site ions) of the apical oxygens are ignored. Solid blue lines are associated with  $(\text{Ca}_{0.1}\text{La}_{0.9})(\text{Ba}_{1.65}\text{La}_{0.35})\text{Cu}_3\text{O}_{7.158}$  and dashed red lines with  $(\text{Ca}_{0.4}\text{La}_{0.6})(\text{Ba}_{1.35}\text{La}_{0.65})\text{Cu}_3\text{O}_{7.174}$ .

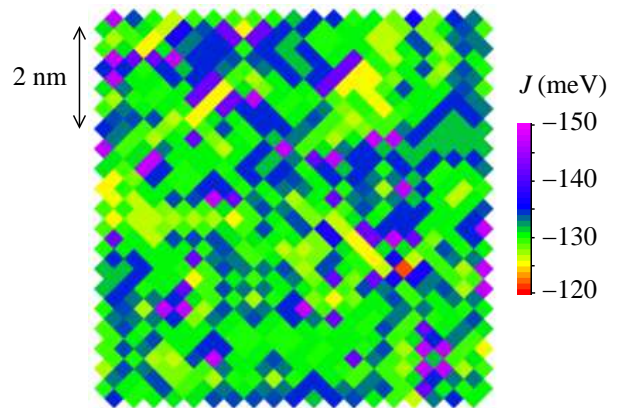


Fig. 3: (Color online) Real-space map of magnetic exchange obtained for a random distribution of the Ba and La ions in the YBCO Ba sites in the  $(\text{Ca}_{0.4}\text{La}_{0.6})(\text{Ba}_{1.35}\text{La}_{0.65})\text{Cu}_3\text{O}_{7.174}$  compound.

Let us now analyze the possible origin of the fluctuations around these average values. The buckling angle and the embedding can be eliminated since they are unique for each compound. The only remaining degrees of freedom are related with the local Ba/La<sub>Ba</sub> distributions. One can think of i) the modification of the apical oxygen ( $O_c$ ) localization as a function of the local Ba/La<sub>Ba</sub> distribution, and ii) the electrostatic potential fluctuations induced by the different  $\text{Ba}^{2+}/\text{La}_{\text{Ba}}^{3+}$  charges. The relative influence of these two degrees of freedom can easily be determined by computing the  $J$  values for each Ba/La<sub>Ba</sub> distributions but with undistorted geometries (see inset of figure 2). Doing so, one sees that i) the  $J$  values still present a large dispersion and ii) that the dispersion range is much larger

(nearly double) than when the apical oxygen displacements are taken into account. It results that contrarily to what is usually admitted, the electrostatic effects play an important role in the effective exchange values. In fact, one of the mayor role of the atomic position relaxation is to moderate this effect. One can thus expect that the actual spatial fluctuations of  $J$  is even larger than the ones calculated in this work and displayed in figure 3. Indeed, not only the electrostatic disorder induced by the Ca/La distribution on the YBCO Y site has not been explicitly taken into account in the present calculations, but in addition there are not any atomic displacement associated with these Ca/La distributions that could soften their electrostatic effects.

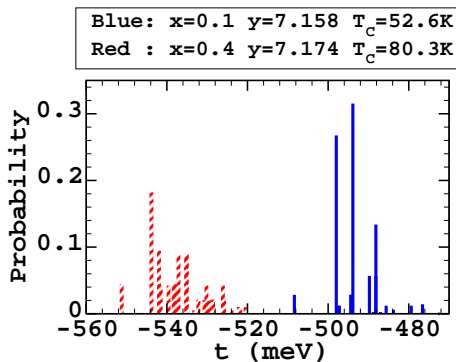


Fig. 4: (Color online) Probability of effective transfer integrals values. Solid blue lines are associated with  $(\text{Ca}_{0.1}\text{La}_{0.9})(\text{Ba}_{1.65}\text{La}_{0.35})\text{Cu}_3\text{O}_{7.158}$  and dashed red lines with  $(\text{Ca}_{0.4}\text{La}_{0.6})(\text{Ba}_{1.35}\text{La}_{0.65})\text{Cu}_3\text{O}_{7.174}$ .

Figure 4 displays the probability of occurrence of the effective hopping values between NN copper atoms. The average transfer for the two compounds  $\bar{t}$  is found to be  $\bar{t}_{x=0.1} = -493$  meV and  $\bar{t}_{x=0.4} = -537$  meV, while the ranges of variation are respectively 36 meV and 37 meV. Basically, the effective transfer integrals behave in a similar way as the effective exchange, both as a function of the buckling angle and of the local electrostatic fluctuations. As far as the on-site repulsion  $U$  is concerned, the system average values are very similar with  $\bar{U}_{x=0.1} = 8.9$  eV and  $\bar{U}_{x=0.4} = 8.8$  eV, and the spatial fluctuations very small in relative values with  $(\Delta U/U)_{x=0.1} = 0.07$  and  $(\Delta U/U)_{x=0.4} = 0.06$ . Let us note that the  $J$  fluctuations nicely agree with their perturbative evaluations from  $t$  and  $U$  fluctuations, that is  $\Delta J \simeq -8(t/U)\Delta t + 4(t/U)^2\Delta U$ .

From the ab initio calculations (excitation spectrum and associated wave functions) one can also derive the difference between nearest neighbor magnetic orbital energies:  $\delta\varepsilon$ . As for the exchange, transfer and on-site Coulomb repulsion the effective energies of the magnetic orbitals do strongly fluctuate in real space. In fact, the orbital energy difference between NN sites is proportional to the difference in the number of Ba/La ions surrounding each copper atom (see figure 5). It comes an energy stabilization of 1.4 eV per additional Ba  $\rightarrow$  La substitution. One

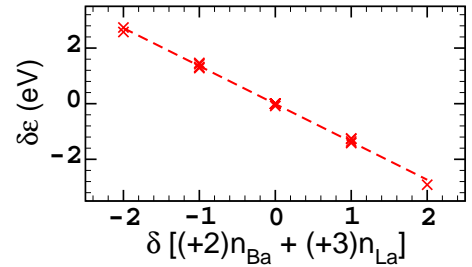


Fig. 5: Magnetic orbital energy difference between NN sites as a function of the charge difference associated with the coppers first neighbors YBCO Ba sites. Crosses: computed points, dashed line: linear fit.

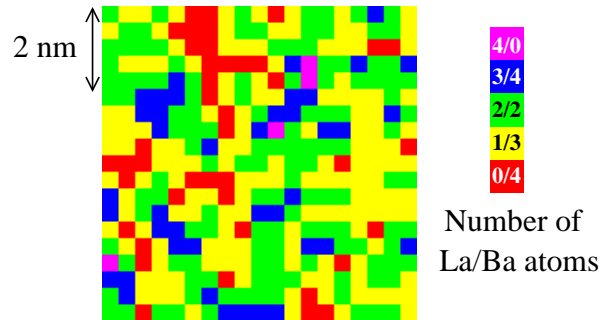


Fig. 6: (Color online) Real-space map of the number of Ba/La ions surrounding a given copper site (or equivalently of the magnetic orbital energy) for a random distribution of the Ba/La atoms in the YBCO Ba sites.

can thus expect an associated real-space electronic density fluctuation as a function of the local ionic configuration. Indeed, our calculations show a correlated fluctuation in the copper atoms population of about  $0.06\bar{c}$ . Figure 6 pictures such an expected fluctuation for a random distribution of the Ba/La atoms in the YBCO Ba sites. The typical scale of the magnetic orbital energies fluctuations and thus of the expected density of states is of the order of a few nanometers.

In summary our calculations showed that the extrinsic inhomogeneities associated with material doping is responsible for both magnetic exchange and on-site orbital energies strong spatial fluctuations. In both cases, the fluctuations are of a typical scale of a few nanometers. First, the computed magnetic orbital energy fluctuations induce an associated fluctuation of the copper density of states and positively correlate (similar typical size and pattern) with the observed LDOS maps as picture in figure 1b of reference [3]. Second, the strong relation between magnetism and superconductivity in high- $T_c$  cuprates [8–11] induces us to compare our exchange fluctuations with the gap inhomogeneities observed in STS experiments [2, 3]. Despite the fact that it relates to different compounds, the typical size of doping inhomogeneities is similar and figure 3 of the present work compares positively with, for instance, figure 1 of reference [4], in all aspects except for the amplitude of the inhomogeneities. However as discussed

above, the electrostatic disorder of the YCBO Y sites was not taken into account and should strongly increase this amplitude. As a matter of example, we computed the  $J$  modification associated with a strongly dissymmetric distribution of the Ca/La ions on the YCBO Y sites and found that the exchange integral is being changed from -146 meV to -98 meV.

In the  $\text{Bi}_2\text{Sr}_2\text{CaCu}_2\text{O}_{8+\delta}$  compounds, the chemical and structural inhomogeneities located close to the superconducting layers are, of course, not due to the counter-ions (as in the present compounds) but rather to the non stoichiometric oxygen atoms. Our results clearly show that this is i) the fluctuations of the apical oxygen location and ii) the local electrostatic environment of the superconducting copper plane that are responsible of the exchange and orbital energy fluctuations. The chemical origin of these structural and electrostatic effects are system dependent, related to doping counter-ions in our case, related to the non stoichiometric oxygen in Bi2212 compounds. In any case our results support the conclusions of McElroy *et al* [17] of an extrinsic (chemical and structural) origin of the gap inhomogeneities and associated critical temperature.

\* \* \*

The authors thank Daniel Maynau for providing them with the CASDI suite of programs. These calculations were done using the CNRS IDRIS computational facilities under project n°1842 and the CRIHAN computational facilities under project n°2007013.

## REFERENCES

- [1] J. G. Bednorz and K. A. Müller, *Z. Phys. B: Condens. Matter* **64**, 189 (1986).
- [2] T. Cren, D. Roditchev, W. Sacks, J. Klein, J.-B. Moussy, C. Deville-Cabellin and M. Lagus, *Phys. Rev. Letters* **84**, 147 (2000).
- [3] S. H. Pan, J. P. O'Neal, R. L. Badzey, C. Chamon, H. Ding, J. R. Engelbrecht, Z. Wang, H. Eisaki, S. Uchida, A. K. Gupta, K.-W. Ng, E. W. Hudson, K. M. Lang and J. C. Davis, *Nature* **413**, 282 (2001).
- [4] K. M. Lang, V. Madhavan, J. E. Hoffman, E. W. Hudson, H. Eisaki, S. Uchida, and J. C. Davis, *Nature* **415**, 412 (2002).
- [5] See for instance : C. Howald, P. Fournier and A. Kapitulnik, *Phys. Rev. B* **64**, 100504 (2001) ; K. M. Lang, V. Madhavan, J. E. Hoffman, E. W. Hudson, H. Eisaki, *Nature* **415**, 412 (2002).
- [6] C. Renner and Ø. Fischer, *Phys. Rev. B* **51**, 9208 (1995).
- [7] J. C. Phillips, A. Saxena and A. R. Bishop, *Rep. Prog. Phys.* **66**, 2111 (2003).
- [8] See for instance : S. S. Kancharla, B. Kyung, D. Sénéchal, M. Civelli, M. Capone, G. Kotliar, and A.-M. S. Tremblay, *Phys. Rev. B* **77**, 184516 (2008).
- [9] See for instance : P. W. Anderson, P. A. Lee, M. Randeria, T.M. Rice, N. Trivedi and F. C. Zhang, *J. Phys.: Condens. Matter* **16**, R755 (2004).
- [10] D. Muñoz, F. Illas and I. de P. R. Moreira, *Phys. Rev. Letters* **84**, 1579 (2000) ; D. Muñoz, I. de P. R. Moreira and F. Illas, *Phys. Rev. B* **65**, 224521 (2002).
- [11] R. Ofer, G. Bazalitsky, A. Kanigel, A. Keren, A. Auerbach, J. S. Lord and A. Amato, *Phys. Rev. B* **74**, 220508 (2006).
- [12] O. Chmaissem, Y. Eckstein and C. G. Kuper, *Phys. Rev. B* **63**, 174510 (2001).
- [13] B. O. Roos, P. R. Taylor and P. E. Siegbahn, *Chem. Phys.* **48**, 157 (1980) ; B. O. Roos, *Advances in Chemical Physics; Ab Initio Methods in Quantum Chemistry*, Part II, vol. **69**, p. 399, John Wiley & Sons Ltd, Chichester, England (1987).
- [14] J. Miralles, J. P. Daudey and R. Caballol, *Chem. Phys. Lett.* **198**, 555 (1992) ; V. M. García *et al.*, *Chem. Phys. Lett.* **238**, 222 (1995) ; V. M. García, M. Reguero and R. Caballol, *Theor. Chem. Acc.* **98**, 50 (1997).
- [15] N. W. Winter, R. M. Pitzer and D. K. Temple, *J. Chem. Phys.* **86**, 3549 (1987).
- [16] A. Gellé and M.-B. Lepetit, *J. Chem. Phys.* **128**, 244716 (2008).
- [17] K. McElroy, Jinho Lee, J. A. Slezak, D.-H. Lee, H. Eisaki, S. Uchida and J. C. Davis, *Science* **309**, 1048 (2005).